IOP Conf. Series: Journal of Physics: Conf. Series **822** (2017) 012003 doi:10.1088/1742-6596/822/1/012003

Experimental investigation of boundary layer transition in flow past a bluff body

Rahul Deshpande

Graduate Student, Department of Aerospace Engineering, Indian Institute of Technology Kanpur, Kanpur, Uttar Pradesh 208016, India

E-mail: raadeshpande@gmail.com

Aditya Desai

Postgraduate Student, Department of Aerospace Engineering, Indian Institute of Technology Kanpur, Kanpur, Uttar Pradesh 208016, India

E-mail: adityad@iitk.ac.in

Vivek Kanti

Project Engineer, National Wind Tunnel Facility, Indian Institute of Technology Kanpur, Kanpur, Uttar Pradesh 208016, India

E-mail: vkanti@iitk.ac.in

Sanjay Mittal

Professor, Department of Aerospace Engineering, Indian Institute of Technology Kanpur, Kanpur, Uttar Pradesh 208016, India

E-mail: smittal@iitk.ac.in

Abstract. We explore the phenomenon of *drag crisis* observed for the flow over bluff bodies at high Reynolds numbers. The drag coefficient reduces significantly beyond a certain Re due to the transition of the boundary layer from laminar to turbulent state. Flow past a smooth sphere and a circular cylinder is experimentally investigated for $1.0 \times 10^5 \leq Re \leq 5.0 \times 10^5$ via unsteady force, surface–pressure and 2–D Particle Image Velocimetry(PIV) measurements. In case of a smooth sphere, the *drag crisis* is observed for $Re > 3.3 \times 10^5$ .The unsteady force measurements reveal that the fluctuations in the force coefficients initially increase with Re in the high subcritical regime and then experience a steep fall in the critical regime. It is found from the PIV measurements that the normal Reynolds stresses in the separated shear layer from the sphere are one order lower in magnitude for the supercritical regime in comparison to the subcritical regime. In the case of flow past a smooth circular cylinder, a two–stage *drag crisis* is captured using surface–pressure measurements where the boundary layer over one side of the cylinder undergoes transition around $Re = 3.9 \times 10^5$ and that over the second side transitions around $Re = 4.8 \times 10^5$. The transition is accompanied with increased fluctuations in the surface–pressure coefficients near the shoulders of the cylinder.

1. Introduction

The phenomenon of boundary layer transition for the flow past a bluff body, popularly called the *drag crisis*, has been of continued interest for the fluid mechanics community. Several numerical and experimental studies have been carried out in the past to characterize the phenomenon and understand the underlying mechanism. During *drag crisis*, the transition of the boundary layer from a laminar to turbulent state causes a very significant reduction in the drag coefficient of the bluff body. The flow separation is delayed due to the increased near-wall momentum. This reduces the size of the wake and increases the base pressure. Here, the drag coefficient is the drag force non–dimensionalized with the dynamic pressure and frontal area of the bluff body. In this work, two bluff bodies are considered: sphere and cylinder. Achenbach[1] proposed dividing the entire $\overline{C}_D$ – Re variation into four flow regimes for flow past a sphere: (i) *subcritical regime* – $\overline{C}_D$ is almost independent of the Reynolds number and maintains a constant value of approximately 0.5, (ii) *critical regime* – a rapid drop in the drag coefficient,i.e., the drag crisis is observed with the $\overline{C}_D$ achieving its minimum value at the critical Reynolds number, (iii) *supercritical regime* – $\overline{C}_D$ increases gradually with Re while the point of transition of the laminar boundary layer to a turbulent state remains fixed at a particular azimuthal angle and (iv) *transcritical regime* – $\overline{C}_D$ increases due to the upstream shift of the point of boundary layer transition with an increase in Re.

Norman and McKeon[2] analyzed the statistics of the force coefficients for the flow over a sphere for $5 \times 10^4 \leq Re \leq 5 \times 10^5$ and observed that the standard deviation of the lateral forces increased rapidly with increasing Re in the subcritical regime. With further increase in Re into the critical regime, the fluctuations jump to a lower value and remain almost constant in the supercritical regime. Their study does not offer any explanation for the abrupt change in the force fluctuations.

One of the earliest and most comprehensive studies on drag crisis of a circular cylinder was carried out by Achenbach[3]. Similar to the flow past a sphere, the flow was classified in different flow regimes on the basis of the nature of the final flow separation from the cylinder surface. He also studied the variation of skin friction drag and pressure drag with Reynolds number and showed that the percentage of skin friction drag in total drag is less than 3% for $6 \times 10^4 \leq Re \leq 5 \times 10^6$. Several experimental and numerical studies have subsequently been carried out to understand the mechanism of drag crisis. Although experiments of different researchers report the onset of the drag crisis in roughly the same range of Reynolds numbers, the discrepancies in the comparison of the mean drag curves indicate that the phenomenon is extremely sensitive to flow conditions and surface roughness.

In the present study, we explore the mechanism for the phenomenon of *drag crisis* via unsteady force, surface–pressure and 2–D PIV measurements for the flow over a smooth sphere and a smooth circular cylinder. We define a sphere/cylinder to be *smooth* if $k/D < 10^{-5}$, where k is the height of the roughness elements on the sphere/cylinder surface and D is the diameter of the sphere/cylinder.

2. Results and Discussions

2.1. Flow past a smooth sphere

Figure 1(a) shows the variation of the time–averaged force coefficients with the Reynolds number. As has been reported in earlier studies, $\overline{C}_D$ is approximately constant in the subcritical regime followed by a rapid decrease in the critical regime. In the supercritical regime, $\overline{C}_D$ is again virtually constant. Although the comparison with results for earlier studies is not shown here, the present results are in excellent agreement with past results ([1],[3]). The lateral force coefficients, $\overline{C}_L$ and $\overline{C}_S$ are negligible in the early subcritical regime and gradually increase as Re approaches the critical Re. Non–zero lateral forces in the critical flow regime were also reported by Norman

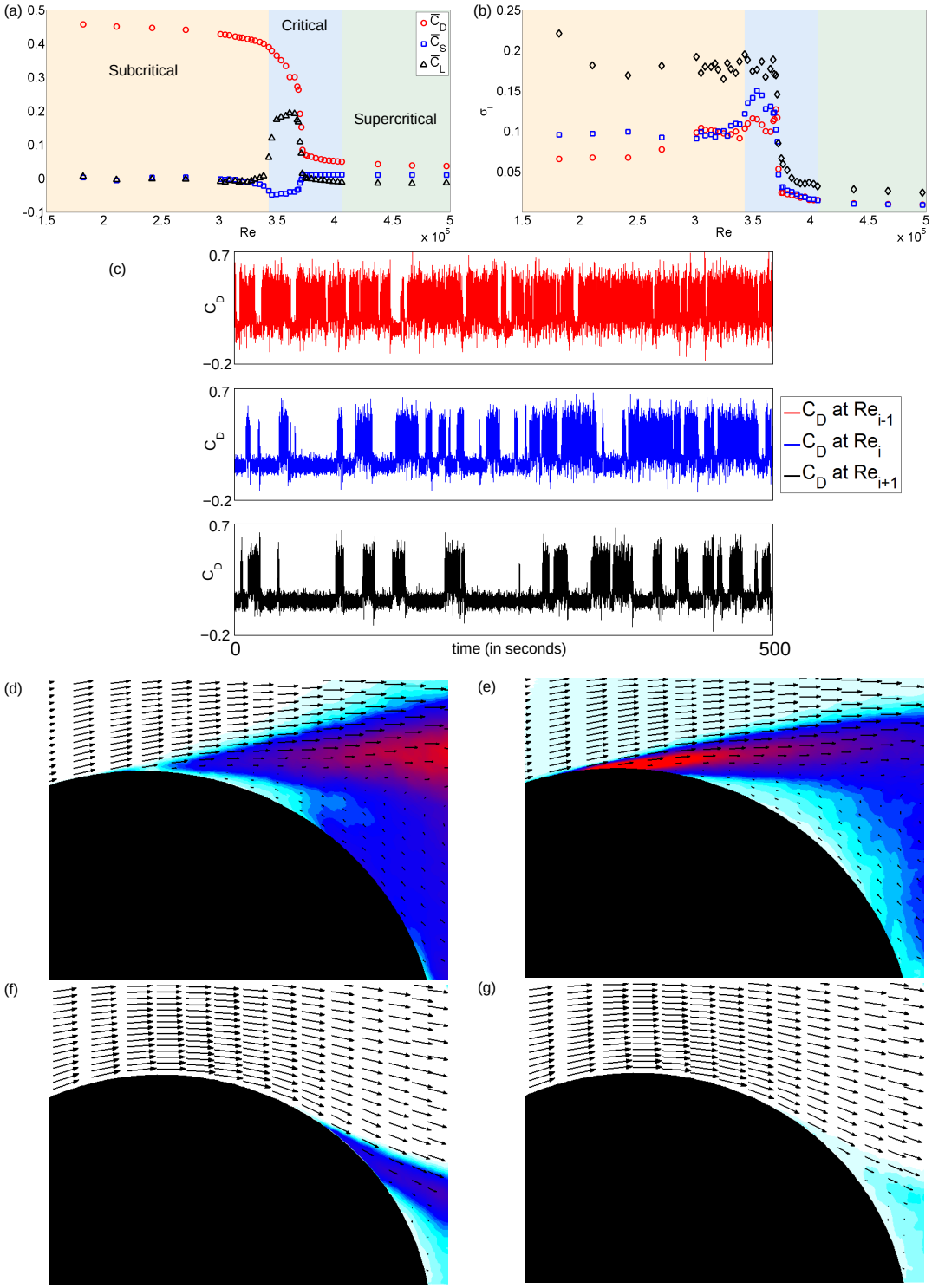

Figure 1. Flow past a sphere: (a)variation of the mean force coefficients with Re. Here, the mean force coefficients represent the time–averaged drag/lateral forces non–dimensionalized with the dynamic pressure and frontal area of the sphere. (b) variation of standard deviation of the force coefficients with Re. (c) C_D time series at three different Re. (d) $\overline{u_r{}'u_r{}'}/U^2{}_\infty$ and (e) $\overline{u_\theta{}'u_\theta{}'}/U^2{}_\infty$ for subcritical $Re = 3.08 \times 10^5$. (f) $\overline{u_r{}'u_r{}'}/U^2{}_\infty$ and (g) $\overline{u_\theta{}'u_\theta{}'}/U^2{}_\infty$ for supercritical $Re = 4.28 \times 10^5$.

and McKeon[3] who attributed it to the minute manufacturing imperfections on the sphere surface. These imperfections result in an earlier boundary layer transition over a particular region of the sphere resulting in a non-axisymmetric flow separation from the sphere surface. As Re approaches the end of the critical regime, the flow transition nears completion throughout the sphere surface due to which the lateral force coefficients decrease in magnitude. In order to check for a bias in the lateral plane, measurements were also carried out after rotating the sphere about the freestream axis at arbitrary angles. Even though the magnitude of $\overline{C}_L$ and $\overline{C}_S$ changed on rotation, the resultant lateral force coefficient remained same at a particular Re, irrespective of the rotations.

The standard deviation of the three force coefficients for various Re is depicted in Figure 1(b). In the subcritical regime, fluctuations in the lift force are almost three times larger than the drag fluctuations. Both the drag and lateral force fluctuations are maximum in the critical regime, with the maximum drag fluctuation occurring at a slightly higher Re as compared to the Re for maximum fluctuation in the lateral forces. On further increasing Re towards the end of the critical regime, these fluctuations decrease in magnitude. In addition, the decrease in the C_L and C_S fluctuations is large and gradual as compared to the jump observed for the fluctuations in C_D. This observation suggests a change in the flow physics near the shoulder of the sphere as the nature of the flow separation from the surface changes from a laminar to turbulent state. The force fluctuations remain nearly constant with Re in the supercritical regime.

To discuss the reason behind the jump in the C_D fluctuations in the critical regime, we show the time series of C_D at three different Re in Figure 1(c). Re_i denotes the Re where the standard deviation in C_D is found to be maximum. Re_{i-1} and Re_{i+1} represent the Reynolds numbers just before and after Re_i where the force measurement was carried out. The C_D time series depicts an intermittent nature at these Re due to the random shift in the C_D between the bistable states in the critical flow regime. For $Re_{i-1} \leq Re \leq Re_{i+1}$, the mean of the higher C_D state is 0.29, while that of the lower state is 0.09, approximately. It can be deduced from the time series data that the higher C_D state exhibits significantly high variation about its mean as compared to the lower C_D state. As we increase the Re from Re_{i-1} towards Re_{i+1}, the probability for the lower C_D state to exist increases as compared to the higher C_D state. The probability of existence of the two states is nearly equal at Re_i leading to the occurrence of maximum fluctuations in C_D. For $Re > Re_{i+1}$, the higher C_D state gradually diminishes. Beyond a certain Re, the lower C_D state is the only observed state. Hence, the standard deviation of C_D falls rapidly on increasing Re beyond Re_i.

To investigate the reason for decrease in lateral force fluctuations, we conducted 2–D Particle Image Velocimetry (PIV) measurements in a planar cut near the sphere surface for both subcritical and supercritical Re. Figures 1(d) and (e) depict the non-dimensionalized radial ($\overline{u_r{'}u_r{'}}/U^2{}_\infty$) and tangential Reynolds stresses ($\overline{u_\theta{'}u_\theta{'}}/U^2{}_\infty$) at a subcritical $Re = 3.08 \times 10^5$. The contour plots depict the unsteadiness after the flow separates as a laminar boundary layer. An increase in magnitude of the radial Reynolds stresses along the separated shear layer suggests increased unsteadiness near the surface of the sphere. Also, the maximum tangential Reynolds stress is observed to be near the shoulder, where the flow separates from the sphere. These stresses eventually decrease in magnitude along the shear layer downstream. The contour plots for the corresponding Reynolds stresses in supercritical regime are shown in Figure 1(f) and (g) at $Re = 4.28 \times 10^5$. In comparison to the laminar flow separation in the subcritical regime, the turbulent separation occurs at a greater azimuthal angle, the wake size is reduced and the unsteadiness close to the sphere surface decreases for the supercritical regime. Figure 1(f) shows that the values of radial Reynolds stresses is moderate along the separated shear layer, while it is low further downstream. Similarly, the tangential Reynolds stress distribution for the supercritical flow regime in Figure 1(g) depicts a decrease in the unsteadiness in the separated shear layer, when compared with the subcritical regime. The comparison between the radial and

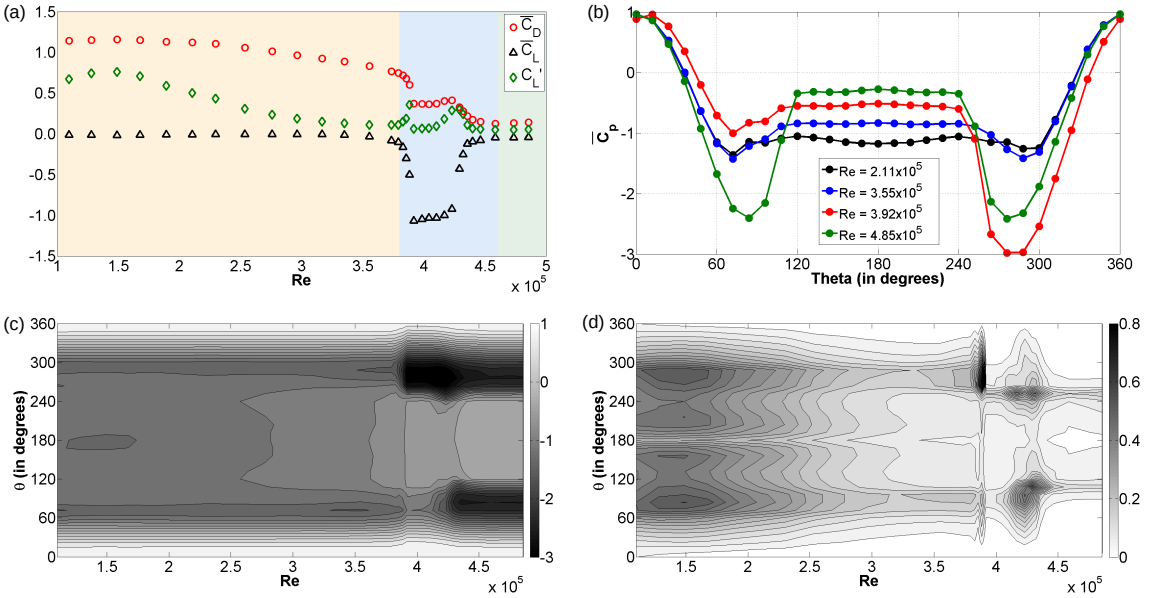

Figure 2. Flow past a circular cylinder: (a) variation of the mean force coefficients ($\overline{C}_D$ and $\overline{C}_L$) and rms of the lift coefficient (C_L') with Re. Here, the force coefficients represent the drag/lateral forces non–dimensionalized with the dynamic pressure and frontal area of the cylinder. (b) $\overline{C}_P$ distribution at selected Re. (c) Angular distribution of $\overline{C}_P$ with Re. (d) Angular distribution of C_P' with Re.

tangential Reynolds stresses shows that the unsteadiness near the sphere surface decreases when the laminar separation changes to a turbulent separation after the drag crisis. This decrease in the unsteadiness near the sphere shoulder can be correlated with the abrupt decrease in the lateral force fluctuations, shown in Figure 1(b), as the Re increases from subcritical to supercritical regime.

2.2. Flow past a smooth circular cylinder

Figure 2(a) shows the variation of aerodynamic force coefficients experienced by the cylinder with Re. The force is obtained by integrating the surface pressure distribution on the cylinder surface. The $\overline{C}_P$ distribution on the cylinder at selected Re are shown in Figure 2(b). Similar to what is observed for a sphere, $\overline{C}_D$ tends to be almost constant upto $Re = 2.3 \times 10^5$,i.e., in the lower subcritical regime. As is seen from the $\overline{C}_P$ distribution, at $Re = 2.11 \times 10^5$, the flow is subcritical over both halves of the cylinder and the flow separates at 84^o, indicating a laminar flow separation from both the sides. As Reynolds number is increased to 3.55×10^5, the separation point moves downstream, to around 108^o along with an increase in the base pressure. A characteristic of the higher subcritical regime for the flow past a circular cylinder is the decrease in the strength of the vortices being shed from the cylinder. This is confirmed by the significant decrease in C_P' and an increase in the base pressure coefficient. Hence, the $\overline{C}_D$ in the higher subcritical regime decreases gradually with increase in Re.

For $Re > 3.8 \times 10^5$, the flow enters the critical regime as the $\overline{C}_D$ starts decreasing rapidly with increase in Re. In the case of a smooth circular cylinder, a two–stage drag crisis is observed along with a large asymmetric state (mean lift) in the critical regime. For convenience, the part of the cylinder between 0^o – 180^o is described as the top side while that between 180^o – 360^o is referred to as the bottom side. At $Re = 3.9 \times 10^5$, the boundary layer over the bottom side of the

cylinder undergoes transition, thus delaying the flow separation on this side till 120^o, while that over the top side remains laminar. This asymmetric flow separation leads to a large mean lift. For the Re where the asymmetric state persists, the circulation associated with this lift leads to a shift in the front stagnation point, as seen in figure 2(b). At $Re = 4.8\times10^5$, the boundary layer over the top side undergoes transition, leading to nearly identical $\overline{C}_P$ distribution on both the sides, with the flow resorting back to the symmetric state (near-zero lift). The two separation points in this regime are located at 120^o, indicating a turbulent flow separation from both the sides.

The contour plots in Figures 2(c) and 2(d) depict the variation of $\overline{C}_P$ and C_P', the root-mean-square fluctuations in C_P with Re and θ. At the onset of the critical regime (around $Re \cong 3.8\times10^5$), C_P' near the bottom shoulder increases significantly, indicating the unsteady dynamics associated with the boundary layer transition. Following this, the -$\overline{C}_P$ (suction) increases on the bottom side. As Re is increased further, transition on the top side results in a significant rise in C_P' near top shoulder followed by an increase in – $\overline{C}_P$.

3. Conclusions

The present study attempts to investigate the *drag crisis* phenomena for flow past a 3-D bluff body(*sphere*) and a 2–D bluff body(*circular cylinder*). The first part of the study explores the variation in the flow physics in the vicinity of a sphere for $1.5 \times 10^5 \leq Re \leq 5.5 \times 10^5$ via unsteady force measurements and 2–D PIV. It was found that the intermittent behavior of C_D in the critical regime first results in the rise and eventually, in the fall of the fluctuations in the drag coefficient, as the Re reaches the end of critical regime. On increasing the Re from subcritical to supercritical regime, our measurements showed that the Reynolds stresses near the sphere surface decrease along with the reduction in the lateral force fluctuations in the critical regime. In the second part of the study, flow over a circular cylinder in the critical regime is investigated using surface pressure measurements. A two–stage drag crisis with each stage corresponding to the boundary layer transition on one side of the cylinder is observed. The boundary layer transition is observed to induce vigorous fluctuations in the surface pressure in the vicinity of the shoulder of the cylinder.

References

[1] Achenbach E.: Experiments on the flow past spheres at very high Reynolds numbers. J. Fluid Mech 54(03):565575, 1972.
[2] Norman A. K., McKeon B. J.: Unsteady force measurements in sphere flow from subcritical to supercritical reynolds numbers. Exp Fluids 51.5:1439-1453, 2011.
[3] Achenbach E.: Distribution of local pressure skin friction around a circular cylinder in cross flow up to $Re = 5 \times 10^5$. J. Fluid Mech 34(04):625-639, 1968.
[4] Norman A. K., Kerrigan E. C., McKeon B. J.: The effect of small amplitude time-dependent changes to the surface morphology of a sphere. J. Fluid Mech 675:268296, 2011.